
High Energy Solar Particles

J. J. Quenby

Phil. Trans. R. Soc. Lond. A 1976 **281**, 491-496

doi: 10.1098/rsta.1976.0045

Email alerting service

Receive free email alerts when new articles cite this article - sign up in the box at the top right-hand corner of the article or click [here](#)

High energy solar particles

BY J. J. QUENBY

Physics Department, Imperial College, London SW7 2AZ

Protons, heavy nuclei and electrons are seen to be emitted from solar flares with energies extending up to the relativistic region. Three different aspects of these observations will be discussed:

(1) Transport processes along magnetic flux tubes in interplanetary space which distort the source spectra and, due to corotation effects, bring different solar source longitudes into view.

(2) Solar longitudinal dependence of the intensity profiles which yields information on energetic particle motion in the corona and the large scale coronal magnetic structure.

(3) Charge composition measurements which show various enhancements of heavy nuclei fluxes relative to normal coronal abundances and thus yield information on the composition and state of ionization of the acceleration region.

1. INTRODUCTION

Solar flares are responsible for the release and possibly the acceleration of energetic charged particles into the solar cavity. Relativistic protons are seen one to three times a year, particularly near solar maximum, but MeV proton events may occur at a rate nearer once per month, again more frequently close to solar maximum. Proton energies can range from below 0.3 MeV to 10 GeV in the most spectacular events while electrons are often seen at 40 keV and occasionally up to 100 MeV (Datlowe, L'Heureux & Meyer 1970). Heavy charged nuclei up to $Z = 44$ have been detected. The energy spectra can usually be represented by a power law in kinetic energy or magnetic rigidity in the higher ranges, but by an exponential law close to 1–10 MeV. Because of the collimating and possible decelerating effect of the interplanetary medium, total energy output from a flare is difficult to estimate from observations at 1 AU,† but figures varying from 5×10^{20} J to 10^{24} J have been given, depending on event size. Correlations between solar energetic particle events and the occurrence of strong type II, III and IV bursts have been noted. Arrival of electrons promptly following the onset of a type III burst, after travelling a distance of 1.2 AU in the interplanetary medium, have been noted at least in the case of the 'scatter free' 40 keV events by Wang, Fisk & Lin 1971. Similarly, prompt onset of protons following the time of maximum of the flash phase has been seen for protons, taking into account a 1.2–1.4 AU travel distance. Generally the bulk of the particles arrive much later, after a diffusive propagation in the interplanetary medium controlled by the field lines connecting the earth to the acceleration region. Low energy particles may remain near 1 AU for more than a week.

In the following we will briefly review three aspects of solar energetic particle observations which eventually lead back to the basic problem of particle acceleration by yielding information on the time history of the particle spectra, the configuration of coronal magnetic fields relevant to particle motion near the Sun and the nuclear composition and state of ionization of the particles at the flare site.

† 1 AU $\approx 15 \times 10^{10}$ m.

2. INTERPLANETARY TRANSPORT PROCESSES

All high energy particles from the Sun reach the Earth guided by the solar wind magnetic field lines. Hence they follow the Parker Archimedes spiral pattern, but the motion is distorted by scattering due to various hydromagnetic waves and discontinuities. As a result, particles arrive easiest from west longitude flares and from a local direction initially $\sim 45^\circ$ W of the Earth–Sun line. The anisotropy is a diffusion current, driven by a peak in flux at the sun near the beginning of an event. Later on, the scattering centres streaming out with the solar wind reduce the near Sun intensity by a combination of convective sweeping and adiabatic deceleration. The deceleration is a result of the expansion of the medium with a net recessional velocity of the scattering centres. When the peak in flux versus radius passes the Earth, the only anisotropy is due to the Compton–Getting transformation of a flux isotropic in the solar wind frame to the Earth frame. Eventually, the anisotropy is directed to the east of the Earth–Sun line as we combine an inward diffusion along the spiral interplanetary field line and the radial outward convection corresponding to the Compton–Getting transformation. The Fokker–Planck transport equation describing these effects is

$$\frac{\delta N}{\delta t} + \frac{1}{r^2} \frac{\delta}{\delta r} (r^2 V N) - \frac{1}{r^2} \frac{\delta}{\delta r} \left(r^2 K_r \frac{\delta N}{\delta r} \right) - \frac{\delta}{\delta T} \left(\frac{dT}{dt} N \right) = 0,$$

where $N(r, t, T)$ is the particle number density at kinetic energy, T and K_r is the radial component of the parallel diffusion coefficient for motion along the mean field lines. $dT/dt = -\frac{4}{3}V/r$ for energy loss in the non-relativistic limit with solar wind velocity V and it is usual to represent $K_r = K_0 r^b$, where r is in AU.

If K_r is very small, diffusion is completely inhibited and the particles are simply convected outward with the solar wind velocity. $V/K_0 = 15 \text{ (AU)}^{b-1}$ or $K_0 = 7.5 \times 10^{19} \text{ cm}^{2-b}/\text{s}$ is the effective limit, below which diffusion dominates. When the diffusion coefficient is small, an additional acceleration is possible if the scattering centres may be represented by waves moving isotropically in the solar wind frame. This is the second order Fermi acceleration. Hence dT/dt in the convective limit is in principle the sum of two terms,

$$\frac{1}{T} \frac{dT}{dt} = 2.25 \frac{V_{A,0}^2}{K_0 r^{b+2}} - \frac{4}{3} \frac{V}{r},$$

where $V_{A,0}$ is the Alfvén speed at the Earth. Supposing an injection into the interplanetary medium at $r = 7R_\odot$ with $V/K_0 = 15 \text{ AU}^{b-1}$, we may draw up the following table comparing the intensity at Earth under combined Fermi acceleration and adiabatic deceleration with that if only the diffusion term were retained in the Fokker–Planck equation.

For $b = -1$: N at Earth is 10^{-3} of diffusive propagation value

For $b = 0$: N at Earth is 10^4 of diffusive propagation value.

For $b = +1$: N at Earth is 10^{60} of diffusive propagation value.

Experimentally we find that many events at the Earth have time profiles which may be explained by velocity dependent diffusion, $K = K(v)$ alone, i.e. no rigidity dependence and small dT/dt . Other events are highly anisotropic for a large part of the time, indicating λ in $K_{11} = \frac{1}{3} \lambda_{\text{mfp}} v$ is given by $\lambda \approx 0.5\text{--}1.0 \text{ AU}$. Thus it is unlikely that the possible gross distortion of the input energy spectra implied by the above table actually take place in interplanetary space and it is reasonable to affirm that we measure spectra representative of those produced within $\sim 10 R_\odot$.

So far we have taken K_0 and b as parameters to be fitted to the data. Attempts to use the well-known plasma-physical quasi-linear theory to deduce K_{11} from measured interplanetary irregularities have not been entirely successful. If it is assumed that all disturbances from the mean Archimedes spiral field are small amplitude transverse waves, scattering may be ascribed to only those waves whose wavelength match the helical motion around the mean field, i.e. such that $k = \omega/v_{11}$. Here ω is the cyclotron frequency. Then diffusion in pitch angle θ ($\cos \theta = \mu$) of the number density $n(z, \mu, t, T)$ is represented for z along \hat{B} by

$$\frac{\delta n}{\delta t} + \mu v \frac{\delta n}{\delta t} = \frac{1}{4} \frac{\delta}{\delta \mu} \left\{ \frac{(1-\mu^2)}{|\mu|v} \frac{e^2}{\mu^2} P_{xx} \left(\frac{\omega}{\mu v} \right) \frac{\delta n}{\delta \mu} \right\},$$

where P_{xx} is evaluated at $k = \omega/\mu v$ and represents the power in transverse waves. K_{11} is related to the inverse of the pitch angle diffusion coefficient. Applying this formalism to a solar proton event on 24 January 1969 where P_{xx} was measured and numerical solutions of the Fokker–Planck were matched to the intensity-time profiles by varying b yielded the following table:

	0.3 MeV	b value		
		1 MeV	5 MeV	10 MeV
region 1	no solution	$-3\frac{1}{2}$	$-2\frac{1}{2}$	$-2\frac{3}{4}$
region 2		no solution		
region 3		no solution		

The table implies that either b is very negative, meaning K_{11} is very large at most $r < 1$ AU, or the value of K_{11} deduced at the Earth from quasi-linear theory is so small that no solution involving diffusive propagation could be found. Thus the general conclusion is that quasi-linear theory underestimates the value of K_{11} obtaining in practice. This might be due to the fact that part of the field fluctuations are in the form of tangential and rotational discontinuities and non-periodic, large amplitude Alfvén waves and hence the theory does not adequately represent the coherence of the field along a particular flux tube that the particle follows. Measurement shows $\langle \delta B^2 \rangle / \langle |B| \rangle \approx 0.3$, rather too high for comfort in a perturbation approach.

Further details of the physics outlined above may be found in McCracken, Rao, Bukata & Keath (1971), Fisk & Axford (1968), Ng & Gleeson (1971), Jokipii, (1971), Webb & Quenby (1973), Webb, Balogh, Quenby & Sear (1973), and Gleeson & Axford (1967).

3. CORONAL TRANSPORT

Solar proton measurements in the 0.3–12 MeV region have yielded a picture of collimated beams, corotating with the Archimedes spiral structure and following in detail the larger distortions of the field from the mean direction. Perpendicular diffusion in interplanetary space is small and the Fokker–Planck equation of §2 applies only in each flux tube. Sometimes $\lambda_{\text{mfp}} \sim 1$ AU. Thus the time history of an event seen by spaceprobes at widely different longitudes can reveal the coronal transport processes from the flare acceleration site because at any instant the spacecraft is connected to unique solar longitude, though of course the temporal history on each flux tube must be taken into account. Employing Pioneers 6, 7, 8 and 9 and observing protons > 10 MeV, McCracken *et al.* found a solar longitude distribution of half width 30° which clearly corotated with the 27 day period.

Roelof *et al.* (1974) have applied a coronal mapping technique to the 2–9 August events. Pioneer 9 and 10 and IMP 5 observations of protons > 13.5 MeV were employed. The proton intensity was plotted against Carrington Longitude on the sun by correcting the solar longitude of the spacecraft by the formula $\Delta\Phi = \Omega r/V$ where V is the measured solar wind speed at r (~ 1 AU) and Ω , the angular solar rotation speed. The plot was compared to a solar magnetic polarity diagram obtained from H α filtergram data. A large connected region of negative polarity lay on the solar equator between Carrington longitudes 90° and 330° (CMP Earth 29 July \rightarrow 7 August 1972) and this correlated with a broad region of peak solar proton intensity as a function of longitude in interplanetary space. Thus it is believed that this polarity cell was responsible for the release of particles into the solar wind. We may note that sector structure boundaries or any well-defined tangential discontinuity is often seen to limit the longitude extent of the solar proton flux.

Simnett (1974) employed Pioneer 6, 7, 8, 9 and IMP 5 observations to study the simultaneous release of protons and electrons at longitude over 100° apart. On 11 August, 1970 at 23h22 U.T. MP 10882 beyond the east limb was responsible for Type IV radio outbursts seen above the limb, hence indicating trapped electrons. Pioneer 7, well connected to this site saw the large interplanetary proton increase, but within a day, spacecraft at many widely separated longitudes saw the event. Meanwhile several optical flares were seen between 12–15 August at MP 10865/68, near the west limb and some overlapped in time with MP 10882 events. The one best correlated with the main event had a dominant non-impulsive X-ray emission and was responsible for the release of electrons and protons seen near the Earth, which had a favourable magnetic connection. The time profiles at the Earth clearly showed energy independence, consistent with a corotation control. Simnett concludes that MP 10882 both released particles beyond the east limb and transported them via closed flux tubes over 100° of longitude to westerly longitudes to cause the event there and the release seen at the Earth.

Reinhard & Wibberenz (1974) have studied the time between flash phase and particle intensity maximum at the Earth, t_n as a function of energy and solar longitude, for many events in the 10–60 MeV proton range. They find that the formula $t_n = c_1(\Phi) + c_2/v$ provides an adequate representation. The second term has $\langle C_2 \rangle = 4.6$ AU and corresponds to velocity dependent diffusion with $\lambda_{\text{mfp}} \sim 0.1$ AU. That is, energy loss is small and the mean free path is large compared to the quasi-linear theory value ~ 0.01 AU at low energies. The first term represents the energy independent coronal diffusion, unlike the second term which corresponds to interplanetary transport. If theories with finite K_\perp (perpendicular diffusion) in interplanetary space were correct, $K_\perp \propto v$ according to all theories, in contradiction to the observed energy independence of $C_1|\Phi|$. Corotation is too slow to account for $C_1|\Phi|$, it actually corresponds to velocities at $1R_\odot$ of 3–12 km/s after corotation correction. It does not explain results in a band 0 – 100° W longitude on the Sun because within this region small t_n values are equally probable and this is thought to be a fast coronal propagation zone. Moreover, there is an element of diffusive propagation in $C_1|\Phi|$ since some prompt particles (rectilinear propagation time) were seen at all longitudes and events to the east outside the fast zone showed a slower rise and fall time than events to the west. However, the basic energy independent coronal transport is ascribed to a $V_D \propto E \times B$ crossed magnetic and electric field drift at $\sim 1R_\odot$, equivalent to plasma motions setting up an electric field $E = -V \times B$.

The fast coronal propagation zone corresponds to some results of Anderson & Lin (1966) who showed that scatter free propagation of 40 keV electrons can occur for events originating

in a solar longitude zone about 100° wide. Of the various theoretical possibilities advanced to explain longitude movement, we can rule out the random walk of flux tubes in interplanetary space which Jokipii & Parker (1967) estimate as being at a rate $\langle(\Delta\Phi)^2\rangle^{\frac{1}{2}} \approx 6\text{--}12^\circ$ in 12 h, clearly too slow. The Fisk–Schatten (1972) idea that a mosaic of neutral lines in the corona transports particles fails in that it requires a reduced field region only 6.7 m thick (\approx particle Larmor radius) for 40 keV electrons and an ambient 1 G (10^{-4} T) field. The Fan *et al.* (1968) suggestion of a fan of field lines spreading out to connect *ca.* 100° of solar wind field to the flare site may work, but perhaps does not necessarily correspond to other coronal information on field structure. Promising is the idea that loops in the field directly transport the particles over $\sim 50^\circ$ longitude, with some small diffusive propagation to move particles from one loop to the next. Thus there is qualitative agreement between the requirements of the energetic particle results and the many other lines of visual and spectroscopic evidence for coronal loop structure extending over many degrees.

4. NUCLEAR COMPOSITION OF ENERGETIC PARTICLE FLUX

There is basic agreement between the nuclear composition of the solar energetic particle flux and the spectroscopic solar abundances, although from flare to flare, a factor two variability in composition may be noticed. This statement is particularly relevant in the 10–100 MeV/nucleon range. Some particular anomalies may occur, for example Si and Mg are over abundant by a factor 5 compared to the oxygen abundance. The ratio Li, Be, B/C, N, O < 0.01 . Most even and a fair number of odd Z elements have been observed up to $Z = 44$.

Below 10 MeV/nucleon an enrichment of high Z material relative to solar abundance is apparent. It increases with decreasing energy, for example Fe/O increases by a factor 2 going down from 10 \rightarrow 1 MeV/nucleon, although a factor 10 variability in this ratio from flare to flare is observed. The enrichment also increases with Z , for example

$$\frac{Z_{\text{s.p.}}}{\text{He}_{\text{s.p.}}} / \frac{Z_{\text{Sun}}}{\text{He}_{\text{Sun}}},$$

where s.p. refers to solar particles, is 10 at $Z = 20$ and 10^3 at $Z = 60$.

Recent experiments with combined solid state detectors and electrostatic analysers (Hoverstadt, Vollmer, Gloeckler & Fan 1973) have shown lack of complete charge stripping at the lowest energies. For instance $C^{+5}/C^{+6} \sim 1.8$ at 100 keV/nucleon and Fe at 2 MeV/nucleon has a charge $Q = 22 \pm 4$.

All the above statements are subject to a solar longitude dependence as the corotation of field lines brings flux tubes with different connection points past the spacecraft, resulting in time variations in the composition ratios.

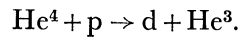
Various theories put forward to explain the low energy enrichment of high Z energetic particles include:

- (a) Preferential escape of partially stripped heavy nuclei from the acceleration region.
- (b) Preferential injection of high Z material into the acceleration region by a Z dependent charge exchange diffusion process.
- (c) Preferential acceleration of partially stripped nuclei in a Fermi acceleration process which has a minimum rigidity for efficient acceleration.

(d) Enrichment of the acceleration region compared with normal coronal material, at the base of the lower corona, as a result of thermal diffusion and gravity settling, although it is not clear why only low energy enrichment results.

Further details of these results may be found in Hoverstadt (1973).

A particular problem in the composition of solar energetic particles is the very large abundance of H^2 , H^3 and He^3 , compared with solar wind and photospheric abundances. This is ascribed to reactions of H^1 and He^4 , e.g.



However, some events with He^3/He^4 large exhibit a complete lack of H^2 and H^3 . Ramaty & Kozlovsky (1974) have made the following arguments to explain the lack of the H^2 and H^3 products expected. They take the August 1972 events in which solar γ -rays were seen at about the same time as accelerated He was measured in the solar particle flux. Accelerated protons hitting the photospheric atmosphere produce neutrons which then react according to $H^1(n, \gamma)H^2$ to give the 2.23 MeV γ line. The He^3/He^4 ratio was consistent with a 2 g/cm^2 path length for relativistic particles and the line emission with a release of 4×10^{30} protons/s in the flare. This latter number checked to an order of magnitude the estimated release based on interplanetary flux measurements. Hence the general scheme of calculation is valid. Now the 2.23 MeV γ line intensity depends on local solar He^3 because some neutrons interact via $He^3(n, p)H^3$ with no radiation. Hence, comparison with other γ line intensities which are not affected by the He^3/H ratio enable a check to be made on the local solar He^3 abundance. This indeed turned out to be consistent with the solar wind measurements. Thus something anomalous in the acceleration process is required for the high He^3/H^1 ratio events. Ramaty *et al.* suggest that if one takes into account the kinematics of He^3 , H^2 and H^3 production down to 0.1 MeV/nucleon, the H^2 and H^3 go forward while the He^3 goes backward. Hence a downward directed proton beam going through $> 10 \text{ g/cm}^2$ photospheric atmosphere, followed by a post-acceleration of the very low energy backward He^3 , enables the solar He^3/H^1 ratio ($= 5 \times 10^{-5}$) to be enhanced. In fact $He^3/H^4 \approx 10^{-3} \rightarrow 1$ can be produced according to Ramaty *et al.* in the accelerated particle flux.

REFERENCES (Quenby)

- Anderson, K. A. & Lin, R. P. 1966 *Phys. Rev. Lett.* **16**, 1121.
 Datlowe, D., L'Heureux, J. & Meyer, P. 1970 *Acta Physica Academiae Scientiarum Hungaricae* **29** (Suppl. 2), 643.
 Fan, C. Y., Pick, M., Pyle, R., Simpson, J. A. & Smith, D. R. 1968 *J. geophys. Res.* **73**, 1555.
 Fisk, L. A. & Axford, W. I. 1968 *J. geophys. Res.* **73**, 4396.
 Fisk, L. A. & Schatten, K. H. 1972 *Solar Phys.* **23**, 204.
 Gleeson, L. J. & Axford, W. I. 1967 *Astrophys. J.* **149**, L115.
 Hovestadt, D., Vollmer, O., Gloeckler, G. & Fan, C. Y. 1973 *Phys. Rev. Lett.* **31**, 650.
 Hovestadt, D. 1973 Rapporteur paper, 13th Int. Conf. Cos. Rays, Denver.
 Jokipii, J. R. & Parker, E. N. 1969 *Astrophys. J.* **155**, 777.
 Jokipii, J. R. 1971 *Rev. Geophys. and Space Phys.* **9**, 27.
 McCracken, K. G., Rao, U. R., Bukata, R. P. & Keath, E. P. 1971 *Solar Phys.* **18**, 100.
 Ng, C. K. & Gleeson, L. J. 1971 *Proc. 12th Int. Conf. Cos. Rays* **2**, 498.
 Ramaty, R. & Kozlovsky, B. 1974 Goddard Space Flight Center preprints X-660-74-94 and X-660-74-255.
 Reinhard, R. & Wibberenz, G. 1974 *Solar Phys.* **36**, 473.
 Roelof, E. C., Lezniak, J. A., Webber, W. R., McDonald, F. B., Teegarden, B. J. & Trainor, J. H. 1974 In *Correlated interplanetary and magnetospheric observations* (ed. D. E. Page), pp. 563–571. Amsterdam: North Holland.
 Simnett, G. 1974 *Solar Phys.* **34**, 377.
 Wang, J. R., Fisk, L. A. & Lin, R. P. 1971 *12th Int. Cos. Ray Conf.*
 Webb, S. & Quenby, J. J. 1973 *Planet Space Sci.* **21**, 23.
 Webb, S., Balogh, A., Quenby, J. J. & Sear, J. F. 1973 *Solar Phys.* **29**, 477